Ind. J. Pharm. Edu. Res., 2026; 60(1):336-347.
https://www.ijper.org

Original Article

Exosomal miR-34b-5p from Bone Marrow Mesenchymal Stem Cells Attenuates Spinal Cord Injury via MAPK/PI3K/AKT Pathway Modulation

Ming Cheng[1], Long Jia[2], Tao Yang[2], Xue Zhou[2], Ling Zeng[2], Hua Lu[3,*], Nianchi Wen[4,*], Benxiang He[5,*]

[1]School of Sports Medicine and Health, Chengdu Sport University, Chengdu, CHINA.
[2]Department of Rehabilitation, Jinniu District People's Hospital, Chengdu, CHINA.
[3]Department of Anesthesia Operation Center, Sichuan Academy of Medical Sciences, Sichuan Provincial People's Hospital, Chengdu, CHINA.
[4]Department of Health Management and Physical Examination, Sichuan Provincial People's Hospital, University of Electronic Science and Technology of China, Chengdu, CHINA.
[5]Party and Government Office, Sichuan Academy of Chinese Medicine Sciences, Sichuan Institute of Chinese Medicine, Chengdu, CHINA.

ABSTRACT

Introduction: Bone Marrow Mesenchymal Stem Cells (BMMSCs) promote Spinal Cord Injury (SCI) recovery via exosomes containing bioactive molecules. This study examined the role and mechanisms of BMMSC-derived exosomes overexpressing microRNA-34b-5p (miR-34b-5p) in neuronal repair after SCI. **Materials and Methods:** BMMSCs were isolated from four 4-week-old Sprague-Dawley rats and introduced to miR-34b-5p mimics or Negative Controls (NC), after which exosomes were extracted and characterized. Twenty-four six-week-old SD rats were assigned to four groups, with 6 rats in each group: Sham, SCI, SCI+NC mimics Exos, and SCI+miR-34b-5p mimics Exos groups. SCI was induced, and exosomes were administered. Histological analysis (HE and Nissl staining), motor function tests (BBB score and horizontal ladder), TUNEL assay, immunofluorescence, ELISA, and Western blotting were performed to evaluate neuronal repair, inflammation, oxidative stress, apoptosis, and signaling pathways. **Results:** SCI resulted in neuronal degeneration, impaired growth, increased apoptosis, and inflammation. BMMSC-derived exosomes overexpressing miR-34b-5p significantly improved neuronal survival ($p<0.01$), reduced apoptosis ($p<0.01$), and mitigated inflammation and oxidative stress ($p<0.05$) compared to controls. Enhanced M2 polarization of microglia was observed ($p<0.01$), alongside inhibition of the MAPK pathway and activation of the PI3K/Akt pathway ($p<0.01$). **Conclusion:** BMMSC-derived exosomes overexpressing miR-34b-5p regulate MAPK and PI3K/Akt pathways, promoting M2 microglial polarization, reducing inflammation and lipid peroxidation, and protecting against neuronal apoptosis in SCI. The findings underscore their efficacy as a therapeutic strategy for SCI.

Keywords: Bone marrow mesenchymal stem cells, Exosome, MiR-34b-5p, Spinal cord injury, MAPK/PI3K/Akt pathway.

Correspondence:

Dr. Benxiang He
Party and Government Office, Sichuan Academy of Chinese Medicine Sciences, Sichuan Institute of Chinese Medicine, No. 51, Section 4, South Renmin Road, Wuhou, Chengdu-610041, CHINA.
Email: hbx202410@163.com

Dr. Hua Lu
Department of Anesthesia Operation Center, Sichuan Academy of Medical Sciences • Sichuan Provincial People's Hospital, No. 32, West Section 2, First Ring Road, Qingyang, Chengdu-610072, CHINA.
Email: 13540895584@163.com

Dr. Nianchi Wen
Department of Health Management and Physical Examination, Sichuan Provincial People's Hospital, University of Electronic Science and Technology of China, No. 32, West Section 2, First Ring Road, Qingyang, Chengdu-610072, CHINA.
Email: 247506854@qq.com

Received: 11-06-2025;
Revised: 29-07-2025;
Accepted: 03-09-2025.

INTRODUCTION

Spinal Cord Injury (SCI) is a challenging and often debilitating condition arising from traumatic or non-traumatic spinal cord damage, typically involving bleeding and ischemia at the affected site, along with movement limitations or potential disability.[1] SCI frequently leads to lifelong impairment and imposes a substantial healthcare burden on patients.[2] Based on pathophysiology, SCI is classified into primary and secondary injuries.[3] Primary injury is the immediate trauma to neurons, glial cells, as well as adjacent vasculature, resulting from compression, shearing, or stretching forces.[4] Secondary injury includes a cascade of detrimental processes, such as neuronal apoptosis, glial scar formation, excitotoxicity, pathological inflammation, ischemia, and localized edema, which worsen neurological function

DOI: 10.5530/ijper.20262022

and extend tissue damage.[5,6] The primary objective in SCI treatment is to preserve remaining core function and restore impaired function. Common interventions include surgery, anti-inflammatory medications, blood pressure management, neuroprotective strategies, and supportive care.[1] Despite these options, the complex pathophysiology of SCI has significantly limited progress in effective treatment development.

Bone Marrow Mesenchymal Stem Cells (BMMSCs) have demonstrated considerable efficacy as a treatment for SCI. However, introducing MSCs directly can lead to adverse reactions, such as immune responses,[7] embolism,[8] secondary infections,[9] and cancer risks.[10] Moreover, most transplanted MSCs gather in organs like the liver, spleen, and lungs, with only a small amount reaching the injury site.[11] Although MSCs are quickly eliminated from the body after systemic administration, the therapeutic effects often remain,[12] suggesting that MSC secretions, particularly exosomes, may drive these effects.[13,14] Recent studies highlight the therapeutic value of MSC-derived exosomes across various neurodegenerative models, including Alzheimer's disease, multiple sclerosis, stroke, neuroinflammation, traumatic brain injury, and SCI.[15] Exosome therapy has shown promise in reducing cell death in SCI models.[16] Additionally, previous findings indicate that exosomes help preserve neurons, offering protection and supporting regeneration of neurons, dendrites, and myelin.[17] Exosomes are also instrumental in limiting scar tissue formation, aiding the regeneration process after SCI.[18]

MicroRNAs (miRNAs) are endogenous, non-coding, single-stranded RNAs, comprising 22 nucleotides, recognized as key biomarkers for diagnosis, prognosis, and therapy. They can impact signaling pathways associated with pathological responses after SCI.[19] MiRNA-34b-5p (miR-34b-5p) has been linked to biological processes including angiogenesis,[20] astrocyte apoptosis,[21] and organ damage.[22] Studies show that silencing miR-34b-5p can alleviate acute lung injury by reducing inflammation and apoptosis.[23] Nonetheless, the precise function of miR-34b-5p in SCI is still not fully defined. Research indicates that exosomes can transport miRNAs, suggesting that BMMSCs may deliver miR-34b-5p via exosomes to aid in SCI treatment. Currently, no studies have explored this specific mechanism. Thus, this study aimed to investigate how exosomes derived from BMMSCs, overexpressing miR-34b-5p, might influence the SCI recovery process.

This study reveals that miR-34b-5p achieves M2 microglial polarization and powerful inhibition of inflammation and oxidative stress by coordinating a dual therapeutic cascade, simultaneously suppressing the pro-inflammatory MAPK pathway and activating the neuroprotective PI3K/Akt axis. This discovery provides an irreplaceable molecular target for the development of miR-34b-5p-based precise intervention diagnosis and treatment strategies.

MATERIALS AND METHODS

Experimental animals

All male Sprague-Dawley rats, aged 4 weeks, were sourced from Chengdu Dashuo Biotechnology Co. Ltd., (Chengdu, China) (License No. SYXK (Sichuan) 2019-0189). Our study was approved by the Experimental Animal Ethics Committee of West China Hospital of Sichuan University (Chengdu, China), Ethics No. 20220713001, and all animal experiments were performed following the Guidelines for the Care and Use of Laboratory Animals. All animals were maintained under standard housing conditions, including 12 hr of alternating light and darkness, humidity controlled between 40% and 60%, a temperature set at 22°C, and unrestricted availability of food and water. Following a week of adaptive feeding, the rats were used for follow-up investigations.

SCI model

Based on a previous study of induced SCI in rat models,[24] these animals were anesthetized by intraperitoneal injection of 1% (w/v) pentobarbital sodium at a dosage of 40 mg/kg. The skin and muscle on the back were incised to expose the spine, followed by removal of the T10 lamina. The surface of the dorsal spinal cord was then fully exposed and subjected to an impact from a stick with a diameter of 2.5 mm and a weight of 10 g, falling from a height of 12.5 mm. Subsequently, the muscles and skin were sutured. To prevent urine from accumulating in the bladder, the rats were manually assisted with urination three times a day until their bladder function was restored to normal levels. The main feature of this sham surgery is that only spinal canal decompression is performed, with no instruments directly touching the dorsal surface of the spinal cord.

All rats were allocated to the Sham group, the SCI group, the SCI+mimics NC Exos group, and the SCI+miR-34b-5p mimics Exos group. For the Sham and SCI groups, the rats were administered a 50 µL injection of PBS into the joint cavity immediately after surgery, as well as on days 3 and 7 post-operation. For the SCI+mimics NC Exos group and the SCI+miR-34b-5p mimics Exos group, equal volumes of BMMSC-Exos (at a concentration of 10^{11} particles/mL) and BMSC-Exos mimic (also at 10^{11} particles/mL) were administered immediately after surgery, and on days 3 and 7 post-surgery. Prior to each injection, the rat's knee joint was flexed at 90° to create additional joint space, and the procedure was carried out along the midline of the patellar tendon to prevent injury to the ligaments within the joint.

Isolation and Characterization of BMSCs

Bone marrow mesenchymal stem cells were isolated following previous studies.[25] In brief, 4-week-old male Sprague-Dawley rats were flushed with DMEM/F12 to collect their bone marrow, which was then separated by centrifugation at 800×g for 5 min. The resulting pellets were collected and plated at a density

of 1×10^6 cells/cm^2 in DMEM/F12 supplemented with 10% heat-inactivated FBS (Sigma-Aldrich, St. Louis, MO, USA), along with 100 U/mL penicillin as well as 100 µg/mL streptomycin (Invitrogen, Carlsbad, CA, USA). The cells were cultured in a controlled environment with humidity, maintained at 37°C and 5% CO_2. Three to four days after the initial plating, the culture medium was changed. Once the cells reached approximately 80-90% confluence, they were subcultured for further growth.

The traditional biomarkers of BMSCs were analyzed using flow cytometry. In summary, we conducted flow cytometric analysis using the following antibodies conjugated with Fluorescein Isothiocyanate (FITC) or Phycoerythrin (PE): CD29, CD90, and CD45 (BioLegend, San Jose, CA, USA). Isotype controls consisted of FITC-IgG, APC-IgG, and PE-IgG immunoglobulins. Following incubation, the cells were rinsed twice and resuspended in FACS buffer for analysis via flow cytometry (BD Biosciences).

Isolation and characterization of exosomes

Extreme centrifugation was used to separate the exosomes. To summarize, we collected the culture supernatant after 48 hr of incubation in FBS-free medium. The culture was then centrifuged at 200 ×g for 10 min at 4°C to eliminate dead cells, at 2000 ×g for 30 min at 4°C to eliminate cell debris, and at 10,000 ×g for 45 min at 4°C to separate broken cells and organelles. The resulting supernatant was filtered through a 0.45 µm membrane to eliminate larger particles. Subsequently, the exosomes were collected by centrifugation at 110,000 ×g for 70 min at 4°C. After centrifugation, the sample was rinsed with PBS and the above centrifugation steps were repeated. Finally, the separated exosomes were resuspended in PBS buffer solution for further analysis.

Transmission Electron Microscopy (TEM) was utilized to assess the morphology and size of the exosomes. In summary, the exosome sample was collected and placed on a carbon-coated copper mesh for 5 min. Any excess liquid was then removed with filter paper. The specimen was treated with a 2% solution of phosphotungstic acid for 2 min. Pictures of the exosomes were subsequently obtained using TEM, and the particle size as well as dispersion were analyzed by Nanoparticle Tracking Analysis (NTA). Exosome-specific markers CD9, CD63, as well as CD81 were detected using Western blot analysis. To quantify the exosomes, the Bicinchoninic Acid (BCA) method was utilized for total protein measurement.

MiRNA Mimics Transfection

MiR-34b-5p mimics (GeneChem, Shanghai, China) were transfected into BMSCs using Lipofectamine 3000 (Thermo Fisher Scientific, USA) according to the protocol. The miR-34b-5p mimics were combined with Lipofectamine 3000 for 20 min before being added to BMSCs for 6 hr. The transfection culture medium was discarded, and entire culture medium was added. The cells were collected after 48 hr.

Real-Time RT-PCR Analysis

RNA was isolated from exosomes with TRIzol reagent (Invitrogen, Carlsbad, CA) as per the instructions. To detect miRNA, we utilized a MiScript reverse transcription kit for the reverse transcription process and applied the miScript SYBR Green (QIAGEN, Hilden, Germany) PCR Kit to quantify the miRNA levels, following the specified volumes and procedures. The reaction mixture, totaling 20 µl, included 10 µl of 2x QuantiTect SYBR Green PCR Master Mix, 0.8 µl of 5M Bulge-Loop™ Reverse Primer, 0.8 µl of 5M Bulge-Loop™ miRNA Forward Primer, 2 µl of cDNA templates (Vazyme, Nanjing, China), and 6.4 µl of RNase-free H_2O. The thermal cycling protocols were set to: 10 min at 95°C, then 45 cycles consisting of 2 seconds at 95°C, 20 sec at 60°C, as well as 10 sec at 70°C. U6 served as the internal reference for miRNA analysis. Data analysis was performed using the $2^{-\Delta\Delta Ct}$ method. MiR-34b-5p is synthesized by Ribo Bio-Tech Co., Ltd. with product number C10211-1.

Functional behaviour evaluation

The locomotor ability was evaluated using the Bresnahan (BBB) scale on days 0, 1, 3, and 7 following SCI. The BBB scale spanned from 0, indicating total paralysis of the hind limbs, to 21, representing normal mobility.[26] To evaluate the stepping and coordination of the forelimbs and hindlimbs, the horizontal step walking test and foot motor function score were performed on rats on the 7th day after SCI, as described in previous studies.[27]

Western blot analysis

RIPA buffer was used to extract total protein from exosomes and tissue samples. Identical quantities of protein extracts (30 µg) were placed into each well and separated using SDS-PAGE. The polypeptides were then moved onto PVDF membranes. After blocking the membranes, rabbit anti-β-actin (1:50,000, Abclonal), rabbit anti-AKT, ERK1/2, JNK1/2, p-AKT, p-ERK1/2, p-JNK1/2 (1:2,000, Abclonal), and rabbit anti-p38 and p-p38 (1:2,000, Bioss) antibodies were added, and the membranes were incubated overnight. Following three rinses with TBST, the membranes were incubated with an HRP-conjugated secondary antibody (Beyotime, 1:5,000) at room temperature for 2 hr. Ultimately, protein expression levels were detected using an enhanced chemiluminescence kit (Millipore). Protein bands were normalized to β-actin as an internal control, and their optical densities were measured, with the ratios calculated.

Evaluation of Spinal Histological Pathology

Morphological detection of the longitudinal section of injured spinal cord using hematoxylin and eosin staining (Richard-Allan Scientific, Kalamazoo, MI, USA) (n=6). Transverse sections were subjected to Nissl staining (cresyl violet, Solarbio) for the

purpose of counting neurons following injury (n=6 per group). The sections underwent standard procedures of deparaffinization, rehydration, and washing. Subsequently, H&E and Nissl staining were executed following the guidelines provided by the manufacturer. In the final step, the sections are dehydrated, fixed, and then mounted on slides with neutral gum. Images were obtained with a Ni-E (Nikon, Tokyo, Japan). The quantity of Nissl bodies was assessed using Nikon NIS Analysis software version 4.54.

Biochemical kit and Enzyme-Linked Immunosorbent Assay (ELISA) detection

The activities of SOD, MDA, CAT, as well as MPO in serum and spinal cord tissues were assessed using biochemical kits, while the levels of TNF-α, IL-1β, and IL-6 in serum and spinal cord tissues were quantified using ELISA kits (Abcam, Cambridge, UK).

TUNEL staining

The TUNEL assay reagent was sourced from Merck KGaA (Darmstadt, Germany). Following the guidelines provided with the kit, TUNEL-positive cells in spinal cord tissues were examined using a microscope. The apoptosis rate is evaluated as follows: TUNEL-positive cell number/total cell number)×100%.

Immunofluorescence

Axon regeneration, neurofilament generation, spinal cord oxidative stress injury and microglia polarization were detected by immunofluorescence assay. Spinal cord tissue was processed as previously outlined and cut into sections of 2.5 μm thickness in either the longitudinal or transverse plane using a Microtome (Leica). After dewaxing, rehydration, and further processing of the sections, the antigens were extracted using citrate buffer (Beyotime, Shanghai, China), and the sections were incubated utilizing 10% goat serum (Solarbio) for blocking. The sample was incubated with these primary antibodies at 4°C overnight: Glial Fibrillary Acidic Protein (GFAP), neurofilament protein (NF), 8-hydroxy-2 deoxyguanosine (8-OHdG), Mitosox, CD16, IBA-α and CD206 (all from Proteintech, Wuhan, Hubei Province, China). After being cleaned, the sections were incubated with the Fluorescein Isothiocyanate (FITC)-conjugated and Tetramethyl Rhodamine Isothiocyanate (TRITC)-conjugated secondary antibodies (Proteintech) for 1 hr at 37°C. DAPI staining was used to observe the nuclei. The microscope (Nikon) was used to take the pictures. Nikon NIS Analysis software, version 4.54, was used to measure the intensity.

miRNA target prediction

First, obtain the targets related to miR-34b-5p from the miRDB and TargetScanHuman databases, and screen the targets related to sci from the Genecard database. Obtain the potential targets by taking the intersection through a Venn diagram. Use the STRING database to construct a Protein-Protein Interaction (PPI) network, and analyze and screen the core targets in the Cytoscape software.

Statistical analysis

IBM SPSS Statistics version 21.0 (IBM Corp.) was used for all statistical analyses. Quantitative results are presented as the Mean±Standard Deviation (SD) derived from a minimum of three experiments. The distinctions among the two groups were evaluated using Student's t-test, whereas variations across several groups were evaluated through One-Way Analysis of Variance (ANOVA). A p-value of less than 0.05 was considered statistically significant.

RESULTS

miR-34b-5p target prediction

Through the miRDB and TargetScanHuman databases, 570 and 2473 miR-34b-5p targets were respectively screened out. Meanwhile, 403 disease-related targets were selected using the Genecard database. The Venn diagram (Figure 1A) analysis results showed that there were 8 potential targets closely related

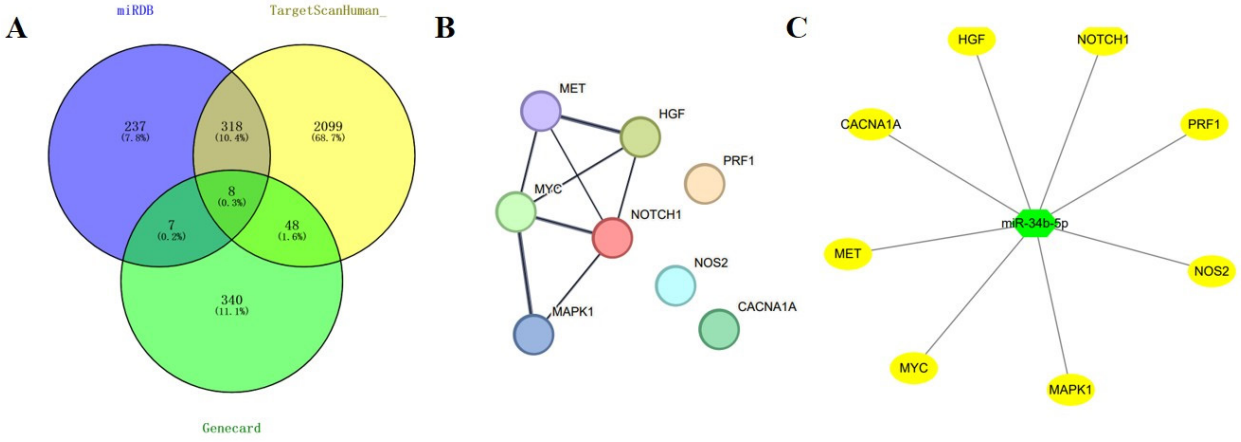

Figure 1: miRNA target prediction. A. Venn diagram. B. PPI network. C. The target network map of miR-34b-5p.

to miR-34b-5p and SCI diseases. Further, a PPI network (Figure 1B) was constructed, and the miR-34b-5p target network diagram was generated with the help of relevant software (Figure 1C).

Production of miR-34b-5p-overexpressing BMMSC-derived exosomes

Firstly, BMMSCs were isolated from the rat bone marrow cavity. Under light microscopy, these cells appeared as elongated, spindle-shaped fibrocyte-like adherent cells (Figure 2A). Fluorescence-Activated Cell Sorting (FACS) revealed that BMMSCs had negative CD45 expression but high levels of CD29 and CD90 (Figure 2B), confirming the successful isolation of BMMSCs.

Next, exosomes were isolated and purified from the BMMSC supernatant using ultracentrifugation and characterized through Transmission Electron Microscopy (TEM), Nanoparticle Tracking Analysis (NTA), and Western blotting. TEM analysis revealed that the vesicles primarily exhibited a characteristic spherical structure with a double membrane, measuring approximately 100 nm in diameter (Figure 2C). NTA analysis indicated a peak size distribution at 141 nm (Figure 2D). Western blot analysis demonstrated a significant increase in exosome marker proteins, such as CD9, CD63, and CD81, in the Exos group than the NC group (Figure 2E), confirming the successful extraction of exosomes from BMMSCs.

Following BMMSC transfection, the miR-34b-5p level was elevated in the miR-34b-5p mimics Exos group compared to the mimics NC Exos group, indicating the successful isolation of exosomes from BMMSCs overexpressing miR-34b-5p (Figure 2F).

Overexpression of miR-34b-5p in BMMSCs-derived exosomes can improve tissue repair and motor function in SCI rats

HE staining was used to investigate pathological changes in spinal cord tissue. In contrast to the Sham group, the SCI group displayed more severe damage, including blurred morphology and structure, extensive necrosis in both gray and white matter, neuronal necrosis and dissolution, loose nerve fibers, cavernous lesions, and microglial proliferation in necrotic areas. In contrast, the SCI+miR-34b-5p mimics Exos group showed clearer delineation between white and red myelin, a higher number of neurons with larger cell bodies, normal cell morphology, and less neuronal degeneration and necrosis, along with minimal glial cell proliferation (Figure 3A).

Nissl staining indicated a marked decrease in neuron count in the SCI group than the Sham group. The SCI+miR-34b-5p mimics Exos group, however, displayed a substantial increase in neuron numbers relative to the SCI+mimics NC Exos group (Figures 3B and 3C) ($p<0.01$).

Regarding locomotor function, the hind limb placement score in the SCI group was notably lower than in the Sham group ($p<0.01$). The SCI+miR-34b-5p mimics Exos group showed an increased hind limb placement score relative to the SCI+mimics

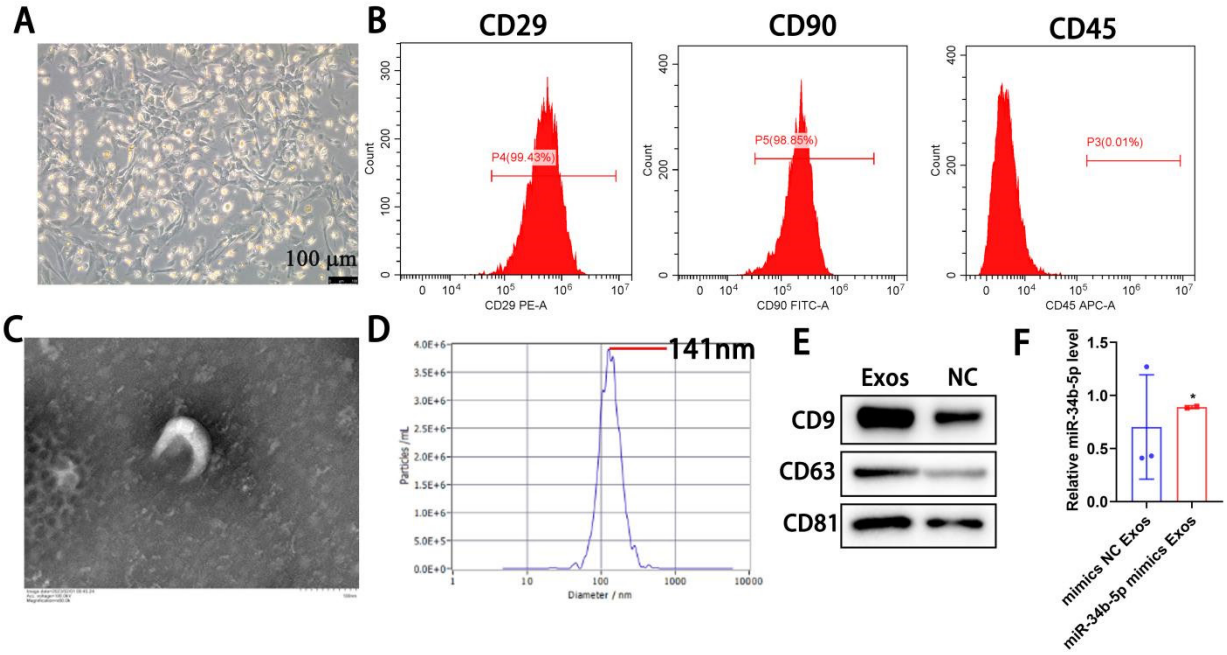

Figure 2: Isolation and identification of BMMSCs and BMMSC-Exos. A. Photoscopic image of bone marrow mesenchymal stem cells (Scale bar: 200 μm); B. The expressions of CD29, CD90 and CD45 were analyzed by flow cytometry; C. Transmission electron microscopy (TEM) image of BMSC-Exos (Scale bar: 100 nm); D. NanoSight tracking analysis (NTA) for the diameters of BMSC-Exo; E. Western blot analysis of CD9, CD63, and CD81; F. The expression of miR-34b-5p was analyzed by fluorescence quantitative PCR. Compared with mimics NC Exos group, *$p<0.05$.

NC Exos group (Figure 3D) ($p<0.05$). Additionally, the BBB score in the SCI group was reduced relative to the Sham group at days 1, 3, and 7 ($p<0.01$). By day 7, the SCI+miR-34b-5p mimics Exos group exhibited a higher BBB score relative to the SCI+mimics NC Exos group (Figure 3E) ($p<0.05$).

These results suggest that exosomes from miR-34b-5p-overexpressing BMMSCs improve tissue repair and locomotor function in rats with SCI.

Overexpressed miR-34b-5p BMMSCs exosomes enhance neuroprotective effects on SCI rats

To evaluate the neuroprotective effects of the intervention on rats with SCI, we assessed neuronal density in the anterior horn of the damaged spinal cord using immunofluorescent staining for GFAP (an astrocyte marker) as well as NF (a neuronal marker). Immunofluorescence results showed that, relative to the Sham group, the SCI group exhibited a substantial reduction in neuronal protein NF expression and a marked increase in astrocyte marker GFAP levels (Figures 4A, 4B, and 4D) ($p<0.01$). In the SCI+miR-34b-5p mimics Exos group, NF expression was significantly upregulated, and GFAP expression was significantly downregulated compared to the SCI+mimics NC Exos group.

Regarding apoptosis in spinal cord tissue, the SCI group displayed a higher rate of TUNEL-positive cells than the Sham group. However, the SCI+miR-34b-5p mimics Exos group displayed a reduction in TUNEL-positive cells relative to the SCI+mimics NC Exos group (Figures 4C and 4E) ($p<0.01$).

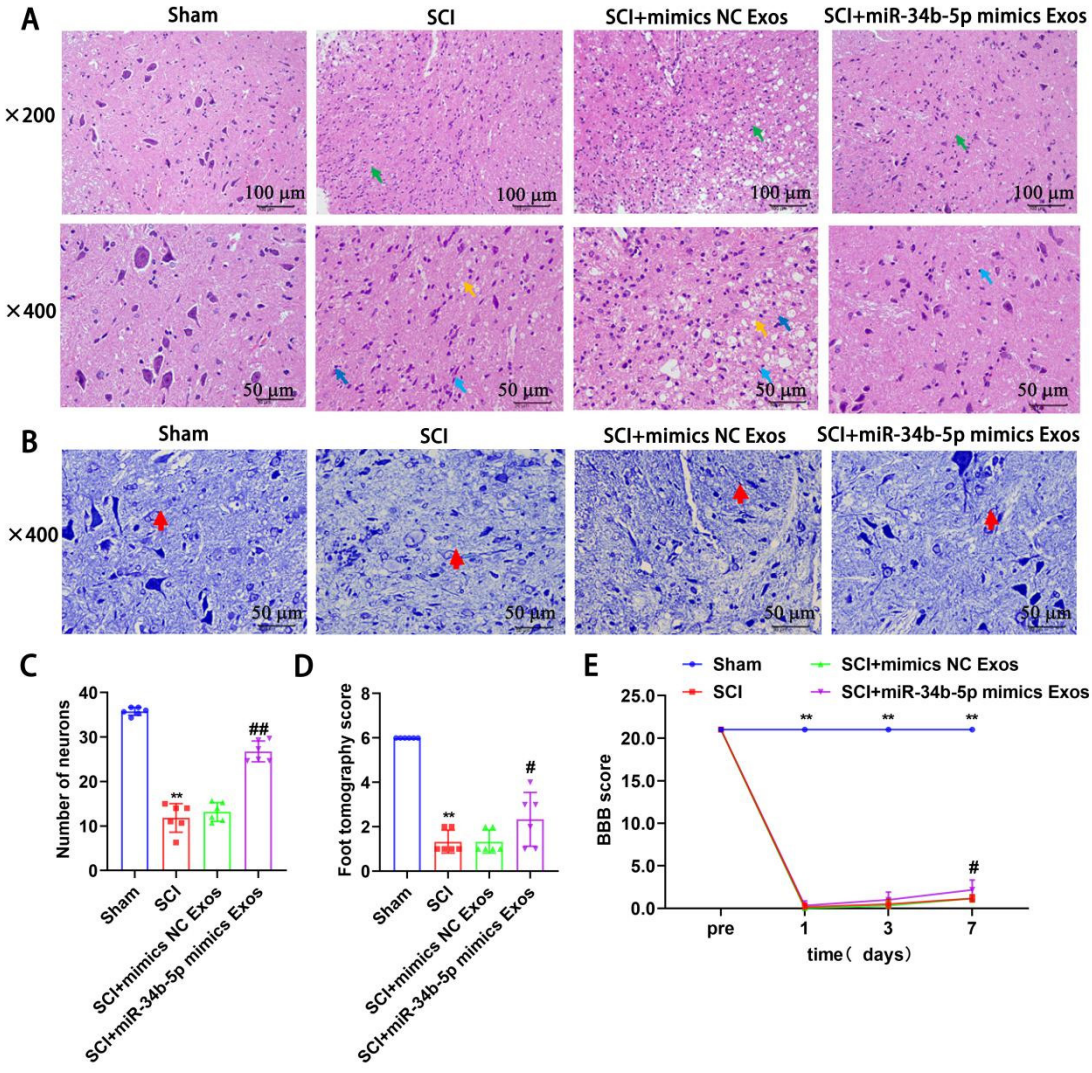

Figure 3: Impact of miR-34b-5p-overexpressing BMMSCs exosomes on tissue injury and locomotor capacity. A. HE staining was used to observe the pathological changes of spinal cord; B. Nissl staining was used to detect the number of surviving neurons; C. Statistical results of the number of neuron cells; D. Horizontal ladder walking assessment score; E. BBB score. Compared with sham operation group, $^{**}p<0.01$; Compared with SCI+mimics NC Exos group: $^{\#}p<0.05$, $^{\#}p<0.05$.

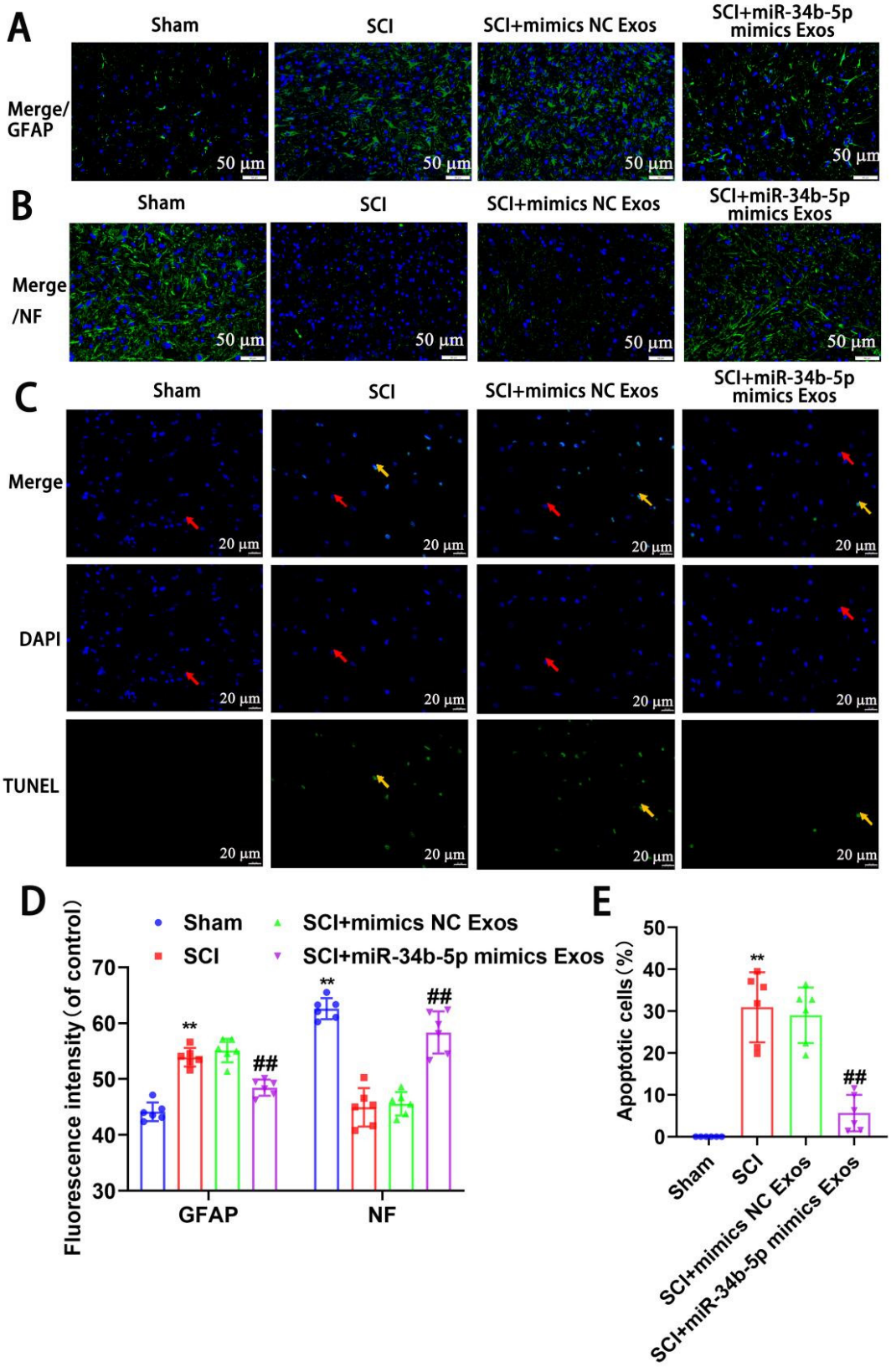

Figure 4: Impact of miR-34b-5p-overexpressing BMSCs exosomes on Neuronogenesis and apoptosis. A. The expression of GFAP was detected by immunofluorescence staining. B. The expression of NF was detected by immunofluorescence staining. C. Apoptosis was detected by flow cytometry; D. Statistical results of immunofluorescence staining. E. Statistical results of apoptosis. Compared with sham operation group, $^{**}p<0.01$; Compared with SCI+mimics NC Exos group, $^{\#}p<0.05$, $^{\#\#}p<0.01$.

Exosomes of BMMSCs overexpressing miR-34b-5p alleviated oxidative stress in SCI rats, regulated microglial polarization, and reduced neuroinflammation

The immunofluorescence results demonstrated that, relative to the Sham group, the expression of oxidative damage marker 8-OHdG as well as mitochondrial superoxide Mitosox were significantly upregulated in the spinal cord tissue of the SCI group ($p<0.01$). However, in the SCI+miR-34b-5p mimics Exos group, the expression levels of 8-OHdG as well as Mitosox were markedly downregulated compared to the SCI+mimics NC Exos group (Figures 5A, 5B, and 5E) ($p<0.05$).

Double immunofluorescent staining revealed that, relative to the Sham group, the expression of CD16 and CD16/IBA-1 were significantly increased, whereas the expression of CD206 and CD206/IBA-1 were notably decreased in the spinal cord tissue of the SCI group ($p<0.01$). In contrast to the SCI+mimics NC Exos group, the SCI+miR-34b-5p mimics Exos group exhibited significantly decreased expression of CD16 and CD16/IBA-1, and significantly increased expression of CD206 and CD206/IBA-1 (Figures 5C-5F) ($p<0.01$).

ELISA analysis showed that, relative to the Sham group, the concentrations of TNF-α, IL-6, IL-1β, MPO, as well as MDA were elevated in both the serum and spinal cord tissues of the SCI group, while the levels of SOD as well as CAT were decreased. In contrast, the SCI+miR-34b-5p mimics Exos group exhibited reduced concentrations of TNF-α, IL-6, IL-1β, MPO, as well as MDA, and increased levels of SOD as well as CAT in both serum and spinal cord tissues relative to the SCI+mimics NC Exos group (Figures 5G-5I) ($p<0.05$).

Exosomes of BMMSCs overexpressing miR-34b-5p inhibit the activation of the MAPK/PI3K/Akt pathway

Western blot analysis revealed that, compared to the Sham group, the levels of p-JNK1/2, p-ERK1/2, and p-p38 were significantly upregulated, whereas the level of p-AKT was markedly downregulated in the SCI group ($p<0.01$). In contrast, the SCI+miR-34b-5p mimics Exos group showed significantly reduced levels of p-JNK1/2, p-ERK1/2, and p-p38, and a marked increase in p-AKT relative to the SCI+mimics NC Exos group ($p<0.01$) (Figure 6).

DISCUSSION

SCI leads to a breakdown in neural connectivity, causing significant and lasting neurological impairment. When SCI occurs, cells in the affected area undergo apoptosis, degeneration, and necrosis, disrupting synaptic connections between neurons and leading to loss of conduction function. In response to the injury, the body initiates self-repair mechanisms, resulting in the proliferation of glial cells, including astrocytes. While these cells play a protective role for neurons, their excessive accumulation forms glial scars at the injury site. These glial scars obstruct the

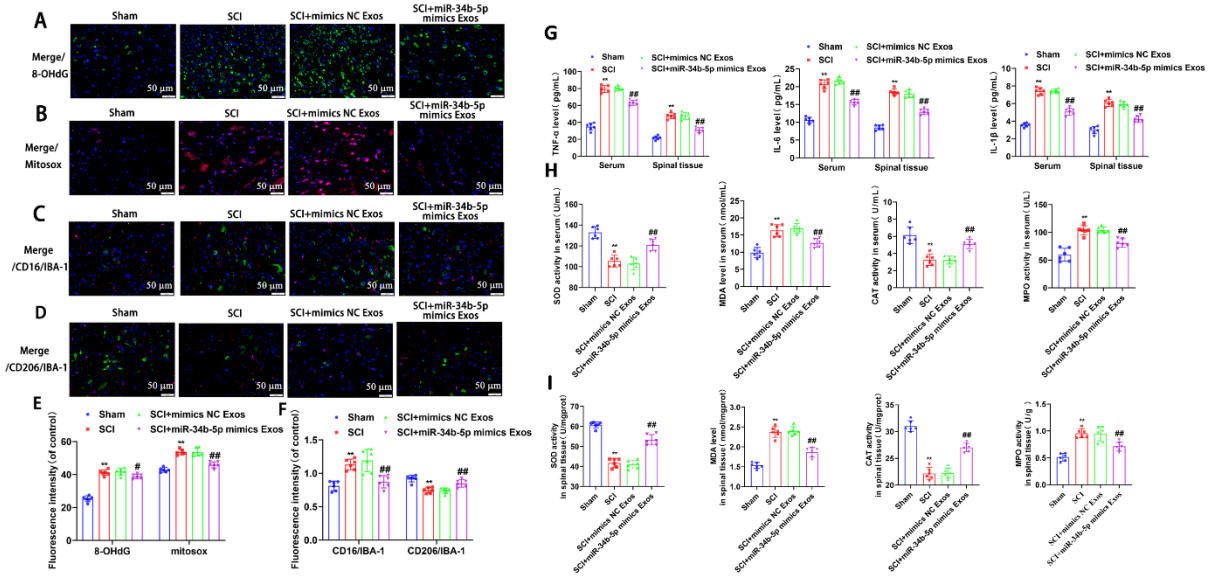

Figure 5: Impact of miR-34b-5p-overexpressing BMSCs exosomes on microglia polarization and oxidative stress. A. The expression of 8-OHdG was detected by immunofluorescence staining. B. The expression of Mitosox was detected by immunofluorescence staining. C. Double immunofluorescence staining was used to detect the expression of CD16/IBA-1. D. Double immunofluorescence staining was used to detect the expression of CD206/IBA-1. E. Statistical results of immunofluorescence staining; F. Statistical results of double immunofluorescence staining. G. The levels of TNF-α, IL-6 and IL-1β in serum and spinal cord tissue were detected by Elisa; H. The activities of MPO, MDA, SOD and CAT in serum were detected by Elisa; I. The activities of MPO, MDA, SOD and CAT in spinal tissue were detected by Elisa. Compared with sham operation group, $^{*}p<0.05$, $^{**}p<0.01$; Compared with SCI+mimics NC Exos group, $^{\#}p<0.05$, $^{\#\#}p<0.01$.

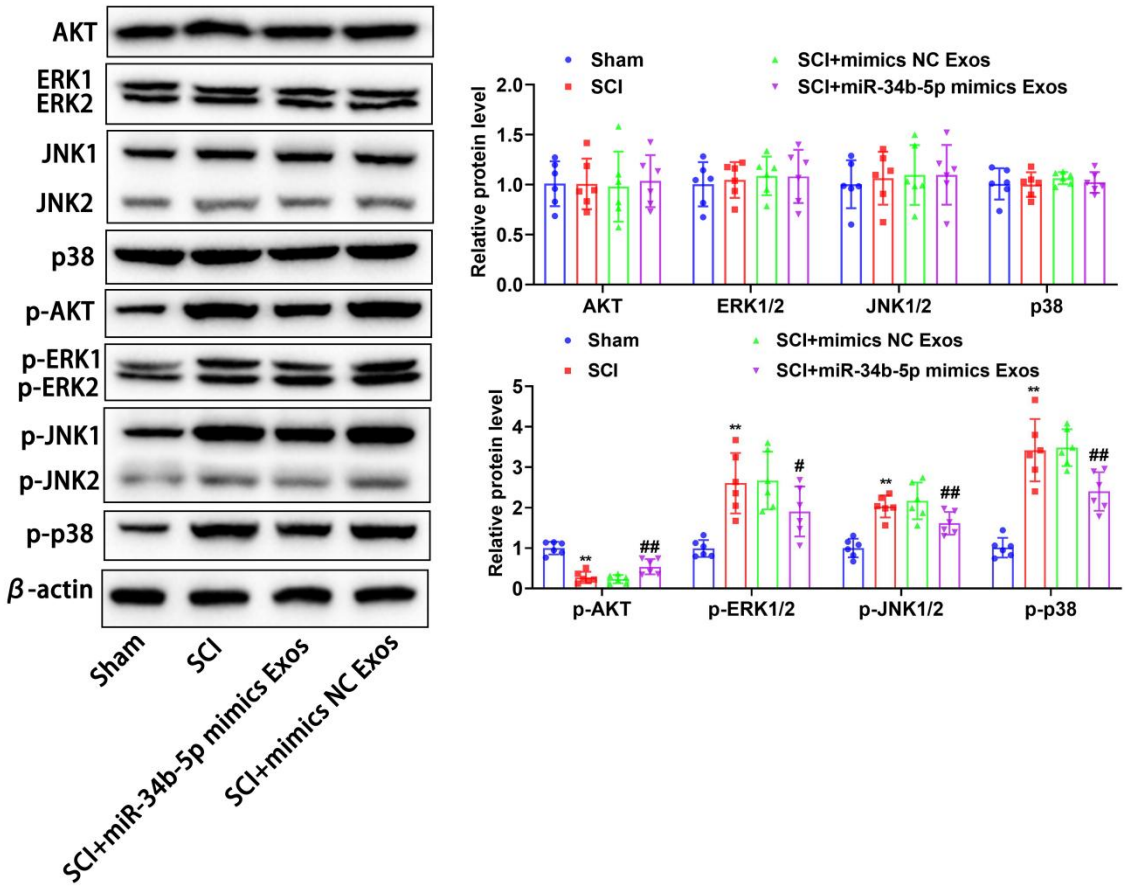

Figure 6: The expression of JNK1/2、p-JNK1/2、ERK1/2、p-ERK1/2、p38、p-p38、AKT、p-AKT in spinal tissue were detected by Western blot. Compared with sham operation group, $^{**}p<0.01$; Compared with SCI+mimics NC Exos group, $^{\#}p<0.05$, $^{\#\#}p<0.01$.

growth of regenerating neurons as well as limit the extension of axons, hindering repair and functional recovery following SCI.

Recent research has shown that miR-34b-5p contributes to the progression of several diseases. For instance, overexpression of miR-34b-5p has been demonstrated to inhibit oxidative stress damage and reduce the proliferation as well as metastasis of breast cancer cells.[28,29] Nevertheless, the contribution of miR-34b-5p in SCI is still underexplored. Our findings indicate that exosomes derived from BMMSCs overexpressing miR-34b-5p can promote neuronal growth and inhibit apoptosis in the spinal cord tissue of SCI rats. Additionally, these exosomes prevent the excessive proliferation of astrocytes, reducing glial scar formation and enhancing motor function recovery in rats with SCI.

Microglial polarization plays a crucial role in the secondary inflammatory damage that follows SCI.[30] During secondary injury, factors such as Reactive Oxygen Species (ROS), lipid peroxidation, as well as inflammation can lead to varying degrees of nerve cell degeneration, apoptosis, and death.[31,32] Activated M1 microglia drive neuroinflammation, which results in neuronal apoptosis and harm to the central nervous system.[33] Promoting the polarization of microglia to the M2 phenotype can reduce inflammation and reverse secondary inflammatory damage.[34] The extent of inflammation following SCI notably impacts the restoration of motor function due to neuronal loss.[35,36]

Recent studies have demonstrated that minimizing apoptosis, degeneration, and necrosis caused by secondary injury, improving the local microenvironment, reducing the release of harmful factors, and fostering favorable conditions for neuronal axon regeneration are effective strategies for enhancing SCI treatment outcomes. Our findings indicate that exosomes from BMMSCs overexpressing miR-34b-5p can alleviate the pathological reactions in the myelin sheath of SCI rats. These exosomes suppress the secretion of pro-inflammatory factors and the activity of lipid peroxidation factors in spinal cord tissue, promote the polarization of microglia to the M2 type, and ultimately prevent nerve cell degeneration and apoptosis.

Secondary damage following SCI involves significant neuroinflammation and neuronal apoptosis, making these processes key targets for treatment.[37,38] However, most therapies tend to address only one of these pathological processes. The MAPK signaling pathway is a primary mechanism mediating the inflammatory response.[39] This pathway regulates the expression of genes associated with inflammation, apoptosis, and cell differentiation through the activation of JNKs, p38,

and ERK cascades.[40] The activation of transcription factors impacts the expression of related genes, influencing the production of pro-inflammatory factors and contributing to neuroinflammation.[41] The activation of MAPK is essential for the synthesis of inflammatory cytokines, like IL-1β as well as IL-6.[42] Inhibiting MAPK pathway can reduce microglia activation, cytokine production, and secondary damage associated with neuroinflammation.[42] Additionally, the MAPK signaling pathway can inhibit neuronal apoptosis by facilitating the polarization of anti-inflammatory M2 microglia.[43] Hence, a promising therapeutic approach is to suppress neuronal inflammation and apoptosis by deactivating MAPK signaling pathways.

The PI3K/Akt signaling pathway plays a role in cell proliferation, differentiation, survival, adhesion, and movement.[44] This pathway is activated under various pathological or stress conditions, such as inflammation, ischemia, hypoxia, and oxidative stress.[45] Akt, a key downstream regulator of PI3K, interacts with various apoptosis-related regulators when activated, promoting cell survival and inhibiting apoptosis.[46] Our findings indicate that BMMSC-derived exosomes overexpressing miR-34b-5p can suppress the activation of the MAPK signaling pathway while enhancing Akt phosphorylation to activate the PI3K/Akt signaling pathway, thus reducing apoptosis.

miR-34b-5p belongs to the miR-34 family and regulates gene expression by binding to the 3'UTR of target mRNAs. Although its core targets have been verified in apoptosis and cancer, bioinformatics predictions (such as TargetScan and miRDB) suggest that it may regulate hundreds of genes, indicating extensive potential off-target effects. To reduce systemic exposure and achieve tissue-specific delivery in future studies, targeted carriers (such as tumor-specific exosomes or antibody-conjugated nanoparticles) can be adopted. Alternatively, specificity can be enhanced and binding to non-target genes can be reduced through chemical modifications.

CONCLUSION

In summary, our findings showed that exosomes from BMMSCs overexpressing miR-34b-5p can promote M2 microglial polarization by modulating the MAPK and PI3K/Akt pathways. This process helps reduce the secretion of inflammatory mediators, prevents neuronal apoptosis, and alleviates oxidative stress. As a result, these exosomes mitigate secondary injury following SCI and support the recovery of motor function. To further validate the therapeutic potential of miR-34b-5p-rich exosomes, future research should expand preclinical testing to larger animal models to better simulate human physiology. Additionally, exploring combination therapies, optimizing drug delivery methods, and evaluating long-term safety profiles are crucial for enhancing the clinical translatability of spinal cord injury treatment.

ABBREVIATIONS

BMMSC: Bone Marrow Mesenchymal Stem Cell; **Exos:** Exosomes; **miR-34b-5p:** MicroRNA-34b-5p; **SCI:** Spinal Cord Injury; **MAPK:** Mitogen-Activated Protein Kinase; **PI3K:** Phosphoinositide 3-Kinase; **Akt:** Protein Kinase B; **HE:** Hematoxylin and Eosin; **BBB:** Basso, Beattie, and Bresnahan Score; **NC:** Negative Control; **TUNEL:** Terminal Deoxynucleotidyl Transferase dUTP Nick End Labeling; **ELISA:** Enzyme-Linked Immunosorbent Assay; **NTA:** Nanoparticle Tracking Analysis; **TEM:** Transmission Electron Microscopy; **SOD:** Superoxide Dismutase; **MDA:** Malondialdehyde; **CAT:** Catalase; **MPO:** Myeloperoxidase; **GFAP:** Glial Fibrillary Acidic Protein; **NF:** Neurofilament Protein; **8-OHdG:** 8-Hydroxy-2'-Deoxyguanosine; **ROS:** Reactive Oxygen Species; **DAPI:** 4',6-Diamidino-2-Phenylindole; **TBST:** Tris-Buffered Saline with Tween-20; **FBS:** Fetal Bovine Serum; **DMEM:** Dulbecco's Modified Eagle Medium; **SPSS:** Statistical Package for the Social Sciences.

CONFLICT OF INTEREST

The authors declare that there is no conflict of interest.

FUNDING

This work was supported by the Sichuan Science and Technology Project (2021YJ0163).

ETHICAL STATEMENT

The experiment was approved by Experimental Animal Ethics Committee of West China Hospital of Sichuan University (Chengdu, China), Ethics number: 20220713001.

AUTHOR CONTRIBUTIONS

BH and HL conceived, designed, and supervised the study and revised the manuscript. MC and LJ performed the experiments, TY provided technical support. BH, HL and MC analyzed the data and edited the manuscript. All authors have read, revised and approved the final version of the manuscript.

SUMMARY

This study investigates the therapeutic role of Bone Marrow Mesenchymal Stem Cell (BMMSC)-derived exosomes enriched with miR-34b-5p in SCI. Exosomes were extracted from BMMSCs transfected with miR-34b-5p mimics and administered to a rat model of SCI. The results demonstrate that these exosomes significantly improve neuronal survival, reduce apoptosis, and mitigate inflammation and oxidative stress by modulating the MAPK and PI3K/Akt pathways. Enhanced M2 microglial polarization and reduced glial scar formation were observed, contributing to motor function recovery. These findings highlight

the potential of miR-34b-5p-enriched exosomes as a promising therapeutic strategy for SCI.

REFERENCES

1. Shao Y, Wang Q, Liu L, Wang J, Wu M. Exosomes from microRNA 146a overexpressed bone marrow mesenchymal stem cells protect against spinal cord injury in rats. J Orthop Sci. 2023; 28(5): 1149-56. doi: 10.1016/j.jos.2022.07.013, PMID 35985935.
2. Karsy M, Hawryluk G. Modern medical management of spinal cord injury. Curr Neurol Neurosci Rep. 2019; 19(9): 65. doi: 10.1007/s11910-019-0984-1, PMID 31363857.
3. Fischer I, Dulin JN, Lane MA. Transplanting neural progenitor cells to restore connectivity after spinal cord injury. Nat Rev Neurosci. 2020; 21(7): 366-83. doi: 10.1038/s41583-020-0314-2, PMID 32518349.
4. Ahuja CS, Nori S, Tetreault L, Wilson J, Kwon B, Harrop J, *et al.* Traumatic spinal cord injury-repair and regeneration. Neurosurgery. 2017; 80(3S):S9-S22. doi: 10.1093/neuros/nyw080, PMID 28350947.
5. Tran AP, Warren PM, Silver J. The biology of regeneration failure and success after spinal cord injury. Physiol Rev. 2018; 98(2): 881-917. doi: 10.1152/physrev.00017.2017, PMID 29513146.
6. Milich LM, Ryan CB, Lee JK. The origin, fate, and contribution of macrophages to spinal cord injury pathology. Acta Neuropathol. 2019; 137(5): 785-97. doi: 10.1007/s00401-019-01992-3, PMID 30929040 [published correction appears in Acta Neuropathol. 2019; 137(5): 799-800. doi: 10.1007/s00401-019-02016-w, PMID 31011858. doi: 10.1007/s00401-019-02016-w].
7. Ma N, Cheng H, Lu M, Liu Q, Chen X, Yin G, *et al.* Magnetic resonance imaging with superparamagnetic iron oxide fails to track the long-term fate of mesenchymal stem cells transplanted into heart. Sci Rep. 2015; 5: 9058. doi: 10.1038/srep09058, PMID 25762186.
8. Cui LL, Kerkelä E, Bakreen A, Nitzsche F, Andrzejewska A, Nowakowski A, *et al.* The cerebral embolism evoked by intra-arterial delivery of allogeneic bone marrow mesenchymal stem cells in rats is related to cell dose and infusion velocity. Stem Cell Res Ther. 2015; 6(1): 11. doi: 10.1186/scrt544, PMID 25971703.
9. Reinders ME, de Fijter JW, Roelofs H, Bajema IM, De Vries DK, Schaapherder AF, *et al.* Autologous bone marrow-derived mesenchymal stromal cells for the treatment of allograft rejection after renal transplantation: results of a phase I study. Stem Cells Transl Med. 2013; 2(2): 107-11. doi: 10.5966/sctm.2012-0114, PMID 23349326.
10. Cai H, Han XJ, Luo ZR, Wang QL, Lu PP, Mou FF, *et al.* Pretreatment with Notoginsenoside R1 enhances the efficacy of neonatal rat mesenchymal stem cell transplantation in model of myocardial infarction through regulating PI3K/Akt/FoxO1 signaling pathways. Stem Cell Res Ther. 2024; 15(1): 419. doi: 10.1186/s13287-024-04039-x, PMID 39533348.
11. Akabane M, Imaoka Y, Kawashima J, Endo Y, Schenk A, Sasaki K, *et al.* Innovative strategies for liver transplantation: the role of mesenchymal stem cells and their cell-free derivatives. Cells. 2024; 13(19): 1604. doi: 10.3390/cells13191604, PMID 39404368.
12. Dadfar S, Yazdanpanah E, Pazoki A, Nemati MH, Eslami M, Haghmorad D, *et al.* The role of mesenchymal stem cells in modulating adaptive immune responses in multiple sclerosis. Cells. 2024; 13(18): 1556. doi: 10.3390/cells13181556, PMID 39329740.
13. Rani S, Ryan AE, Griffin MD, Ritter T. Mesenchymal stem cell-derived extracellular vesicles: toward cell-free therapeutic applications. Mol Ther. 2015; 23(5): 812-23. doi: 10.1038/mt.2015.44, PMID 25868399.
14. Ng KS, Kuncewicz TM, Karp JM. Beyond hit-and-run: stem cells leave a lasting memory. Cell Metab. 2015; 22(4): 541-3. doi: 10.1016/j.cmet.2015.09.019, PMID 26445510.
15. Guy R, Offen D. Promising opportunities for treating neurodegenerative diseases with mesenchymal stem cell-derived exosomes. Biomolecules. 2020; 10(9): 1320. doi: 10.3390/biom10091320, PMID 32942544.
16. Lu Y, Zhou Y, Zhang R, Wen L, Wu K, Li Y, *et al.* Bone mesenchymal stem cell-derived extracellular vesicles promote recovery following spinal cord injury via improvement of the integrity of the blood-spinal cord barrier. Front Neurosci. 2019; 13: 209. doi: 10.3389/fnins.2019.00209, PMID 30914918.
17. Wang L, Pei S, Han L, Guo B, Li Y, Duan R, *et al.* Mesenchymal stem cell-derived exosomes reduce A1 astrocytes via downregulation of phosphorylated NFκB P65 subunit in spinal cord injury. Cell Physiol Biochem. 2018; 50(4): 1535-59. doi: 10.1159/000494652, PMID 30376671.
18. Liu W, Wang Y, Gong F, Rong Y, Luo Y, Tang P, *et al.* Exosomes derived from bone mesenchymal stem cells repair traumatic spinal cord injury by suppressing the activation of A1 neurotoxic reactive astrocytes. J Neurotrauma. 2019; 36(3): 469-84. doi: 10.1089/neu.2018.5835, PMID 29848167.
19. Tigchelaar S, Streijger F, Sinha S, Flibotte S, Manouchehri N, So K, *et al.* Serum microRNAs reflect injury severity in a large animal model of thoracic spinal cord injury. Sci Rep. 2017; 7(1): 1376. doi: 10.1038/s41598-017-01299-x, PMID 28469141.
20. Maroof H, Islam F, Ariana A, Gopalan V, Lam AK. The roles of microRNA-34b-5p in angiogenesis of thyroid carcinoma. Endocrine. 2017; 58(1): 153-66. doi: 10.1007/s12020-017-1393-3, PMID 28840508.
21. Liu L, Liu L, Shi J, Tan M, Xiong J, Li X, *et al.* MicroRNA-34b mediates hippocampal astrocyte apoptosis in a rat model of recurrent seizures. BMC Neurosci. 2016; 17(1): 56. doi: 10.1186/s12868-016-0291-6, PMID 27514646.
22. Qiu N, Xu X, He Y. LncRNA TUG1 alleviates sepsis-induced acute lung injury by targeting miR-34b-5p/GAB1. BMC Pulm Med. 2020; 20(1): 49. doi: 10.1186/s12890-020-1084-3, PMID 32087725.
23. Xie W, Lu Q, Wang K, Lu J, Gu X, Zhu D, *et al.* miR-34b-5p inhibition attenuates lung inflammation and apoptosis in an LPS-induced acute lung injury mouse model by targeting progranulin. J Cell Physiol. 2018; 233(9): 6615-31. doi: 10.1002/jcp.26274, PMID 29150939.
24. Gu J, Jin ZS, Wang CM, Yan XF, Mao YQ, Chen S. Bone marrow mesenchymal stem cell-derived exosomes improves spinal cord function after injury in rats by activating autophagy. Drug Des Dev Ther. 2020; 14: 1621-31. doi: 10.2147/DDDT.S237502, PMID 32425507.
25. Li R, Zhao K, Ruan Q, Meng C, Yin F. Bone marrow mesenchymal stem cell-derived exosomal microRNA-124-3p attenuates neurological damage in spinal cord ischemia-reperfusion injury by downregulating Ern1 and promoting M2 macrophage polarization. Arthritis Res Ther. 2020; 22(1): 75. doi: 10.1186/s13075-020-2146-x, PMID 32272965.
26. Chen H, Zhao H. Resveratrol enhances the efficacy of combined BM-MSCs therapy for rat spinal cord injury via modulation of the Sirt-1/NF-κB signaling pathway. Neurochem Res. 2024; 50(1): 12. doi: 10.1007/s11064-024-04264-z, PMID 39549125.
27. Fan F, Yin T, Wu B, Zheng J, Deng J, Wu G, *et al.* The role of spinal neurons targeted by corticospinal neurons in central poststroke neuropathic pain. CNS Neurosci Ther. 2024; 30(6): e14813. doi: 10.1111/cns.14813, PMID 38887838.
28. Das S, Rai SN. Predicting the effect of miRNA on gene regulation to foster translational multi-omics research-A review on the role of super-enhancers. Noncoding RNA. 2024; 10(4): 45. doi: 10.3390/ncrna10040045, PMID 39195574.
29. Dong L, Chen F, Fan Y, Long J. MiR-34b-5p inhibits cell proliferation, migration and invasion through targeting ARHGAP1 in breast cancer. Am J Transl Res. 2020; 12(1): 269-80. PMID 32051752.
30. Lin J, Pan X, Huang C, Gu M, Chen X, Zheng X, *et al.* Dual regulation of microglia and neurons by Astragaloside IV-mediated mTORC1 suppression promotes functional recovery after acute spinal cord injury. J Cell Mol Med. 2020; 24(1): 671-85. doi: 10.1111/jcmm.14776, PMID 31675186.
31. Zhang Q, Zhang L, Lin G, Luo F. The protective role of vagus nerve stimulation in ischemia-reperfusion injury. Heliyon. 2024; 10(10): e30952. doi: 10.1016/j.heliyon.2024.e30952, PMID 38770302.
32. Liang Y, Feng Q, Wang Z. Mass spectrometry imaging as a new method: to reveal the pathogenesis and the mechanism of traditional medicine in cerebral ischemia. Front Pharmacol. 2022; 13: 887050. doi: 10.3389/fphar.2022.887050, PMID 35721195.
33. He L, Huang G, Liu H, Sang C, Liu X, Chen T. Highly bioactive zeolitic imidazolate framework-8-capped nanotherapeutics for efficient reversal of reperfusion-induced injury in ischemic stroke. Sci Adv. 2020; 6(12): eaay9751. doi: 10.1126/sciadv.aay9751, PMID 32206718.
34. Liu W, Xu B, Xue W, Yang B, Fan Y, Chen B, *et al.* A functional scaffold to promote the migration and neuronal differentiation of neural stem/progenitor cells for spinal cord injury repair. Biomaterials. 2020; 243: 119941. doi: 10.1016/j.biomaterials.2020.119941, PMID 32172034.
35. Wang C, Gong Z, Huang X, Wang J, Xia K, Ying L, *et al.* An injectable heparin-laponite hydrogel bridge FGF4 for spinal cord injury by stabilizing microtubule and improving mitochondrial function. Theranostics. 2019; 9(23): 7016-32. doi: 10.7150/thno.37601, PMID 31660084.
36. Wang C, Wang Q, Lou Y, Xu J, Feng Z, Chen Y, *et al.* Salidroside attenuates neuroinflammation and improves functional recovery after spinal cord injury through microglia polarization regulation. J Cell Mol Med. 2018; 22(2): 1148-66. doi: 10.1111/jcmm.13368, PMID 29148269.
37. Hong JY, Davaa G, Yoo H, Hong K, Hyun JK. Ascorbic acid promotes functional restoration after spinal cord injury partly by epigenetic modulation. Cells. 2020; 9(5): 1310. doi: 10.3390/cells9051310, PMID 32466098.
38. Wang D, Wang K, Liu Z, Wang Z, Wu H. Valproic acid-labeled chitosan nanoparticles promote recovery of neuronal injury after spinal cord injury. Aging (Albany, NY). 2020; 12(10): 8953-67. doi: 10.18632/aging.103125, PMID 32463791.
39. Tan L, Li J, Wang Y, Tan R. Anti-neuroinflammatory effect of alantolactone through the suppression of the NF-κB and MAPK signaling pathways. Cells. 2019; 8(7): 739. doi: 10.3390/cells8070739, PMID 31323885.
40. Sun Y, Liu WZ, Liu T, Feng X, Yang N, Zhou HF. Signaling pathway of MAPK/ERK in cell proliferation, differentiation, migration, senescence and apoptosis. J Recept Signal Transduct Res. 2015; 35(6): 600-4. doi: 10.3109/10799893.2015.1030412, PMID 26096166.
41. Lee SG, Rod-In W, Jung JJ, Jung SK, Lee SM, Park WJ. Lipids extracted from Aptocyclus ventricosus Eggs possess immunoregulatory effects on RAW264.7 cells by activating the MAPK and NF-κB signaling pathways. Mar Drugs. 2024; 22(8): 368. doi: 10.3390/md22080368, PMID 39195484.
42. Yuan Y, Long H, Zhou Z, Fu Y, Jiang B. PI3K-AKT-Targeting breast cancer treatments: natural products and synthetic compounds. Biomolecules. 2023; 13(1): 93. doi: 10.3390/biom13010093, PMID 36671478.
43. Xiao S, Wang C, Yang Q, Xu H, Lu J, Xu K. Rea regulates microglial polarization and attenuates neuronal apoptosis via inhibition of the NF-κB and MAPK signalings for spinal cord injury repair. J Cell Mol Med. 2021; 25(3): 1371-82. doi: 10.1111/jcmm.16220, PMID 33369103.

44. Guo J, Dai X, Laurent B, Zheng N, Gan W, Zhang J, *et al.* AKT methylation by SETDB1 promotes AKT kinase activity and oncogenic functions. Nat Cell Biol. 2019; 21(2): 226-37. doi: 10.1038/s41556-018-0261-6, PMID 30692625.

45. Li X, Hu X, Wang J, Xu W, Yi C, Ma R, *et al.* Short-term hesperidin pretreatment attenuates rat myocardial ischemia/reperfusion injury by inhibiting high mobility group box 1 protein expression via the PI3K/Akt pathway. Cell Physiol Biochem. 2016; 39(5): 1850-62. doi: 10.1159/000447884, PMID 27744432.

46. Jahan S, Ansari UA, Srivastava AK, Aldosari S, Alabdallat NG, Siddiqui AJ, *et al.* A protein-miRNA biomic analysis approach to explore neuroprotective potential of nobiletin in human neural progenitor cells (hNPCs). Front Pharmacol. 2024; 15: 1343569. doi: 10.3389/fphar.2024.1343569, PMID 38348393.

Cite this article: Cheng M, Jia L, Yang T, Zhou X, Zeng L, Lu H, *et al*. Exosomal miR-34b-5p from Bone Marrow Mesenchymal Stem Cells Attenuates Spinal Cord Injury via MAPK/PI3K/AKT Pathway Modulation. Indian J of Pharmaceutical Education and Research. 2026;60(1):336-47.